PROTEINS: Structure, Function, and Bioinformatics 59:489–495 (2005)

Quantum Study of Mutational Effect in Binding of Efavirenz to HIV-1 RT

Ye Mei,[1] Xiao He,[1] Yun Xiang,[2] Da W. Zhang,[2] and J.Z.H. Zhang[1,2]
[1]*Institute of Theoretical and Computational Chemistry, Key Laboratory of Mesoscopic Chemistry and Jiangsu Provincial Laboratory for Nano-Technology, College of Chemistry and Chemical Engineering, Nanjing University, Nanjing, China*
[2]*Department of Chemistry, New York University, New York*

ABSTRACT **Full quantum mechanical computational study has been carried out to study binding of efavirenz (EFZ), a second generation FDA approved nonnucleoside inhibitor, to HIV-1 reverse transcriptase (RT) and its K103N and Y181C mutants using the MFCC (molecular fractionation with conjugate caps) method. The binding interaction energies between EFZ and each protein fragment are calculated using a combination of HF/3-21G, B3LYP/6-31G* and MP2/6-31G* ab initio levels. The present computation shows that Efavirenz binds to HIV-1 RT predominantly through strong electrostatic interaction with the Lys101 residue. The small loss of binding to K103N mutant by Efavirenz can be attributed to a slightly weakened attractive interaction between the drug and Lys101 due to a conformational change of mutation. The small loss of binding to Y181C mutant by efavirenz can be attributed to the Glu698 residue moving closer to EFZ due to conformational change, which results in an increase of repulsive energy relative to the wild type (WT). The binding of efavirenz-derived DPC961 to HIV-1 RT is enhanced by an additional attractive interaction to residue Hid235 and reduced repulsion to Glu698, resulting in an increase of binding energy by about 4 kcal/mol. Proteins 2005;59:489–495.**

INTRODUCTION

HIV-1 reverse transcriptase (RT) is responsible for the conversion of single-stranded viral RNA into double-stranded DNA prior to integration into the genome of the human host.[1] The RT is an excellent target for drug design because it is essential for HIV replication but is not required for normal cell replication. The nonnucleoside analogue inhibitors (NNRTIs) bind to the allosteric position approximately 10 Å from the active site and cause displacement of catalytic aspartate triad.[2–7] Nonnucleoside inhibitors of RT are especially attractive drug candidates because they do not function as chain terminators and do not bind at the dNTP site,[8,9] making them less likely to interfere with the normal function of other DNA polymerase and therefore less toxic than nucleoside inhibitors (NRTIs) such as AZT. The NNRTIs analog such as nevirapine and Efavirenz are noncompetitive inhibitors that lock the polymerase active site in an inactive conformation and cause inhibition by allosteric modifications.[10–13]

Although NNRTIs are highly specific and less toxic than nucleoside inhibitors, their therapeutic effectiveness is limited by relatively rapid emergence of drug-resistant HIV-1 strains. The first-generation NNRTIs, such as nevirapine and delavirdine, show orders of magnitude decrease in binding affinity as a result of many single point mutations in RT.[14] Our previous quantum computational study for nevirapine binding to RT showed that the loss of binding of nevirapine to RT mutation is directly related to the weak binding profile.[15] Without any strong hydrogen bonding between RT and nevirapine, the binding energy between RT and nevirapine is decreased by about 14 kcal/mol with K103N mutation and a further loss of about 8 kcal/mol with Y181C mutation at the HF/3-21G level of ab initio calculation.[15] The computed decrease in binding energy of nevirapine is in strong correlation with the experimentally observed 40-fold loss of binding to K103N mutant and 113-fold loss to Y181C mutant. EFZ belongs to the so-called second-generation NNRTIs that have a more favorable resistance profile, showing smaller losses of activity against many common drug-resistance mutations.[16] Thus, understanding the binding mechanism of EFZ to RT and its mutations is extremely useful to help develop new and more potent mutation-resistant inhibitors. In this respect, quantum computational study could play a unique role in the study of EFZ binding to RT.

HIV-1 RT is a heterodimer with P66 and P51 subunits. P66 contains two domains, the N-terminal polymerase domain (440 amino acids) and the C-terminal RNase H domain (120 residues). P51 contains only the N-terminal polymerase domain. Due to large size of the enzyme, computational studies of RT-drug binding are primarily based on a molecular mechanics approach.[17–19] Recently, a hybrid quantum mechanical/molecular mechanics (MM/QM) study for binding of nevirapine to HIV-1 RT was reported by Kuno et al. and obtained useful information about the stacking interaction.[20] A full quantum study of nevirapine binding to RT using the MFCC approach was recently completed.[15] In that study, binding energy of nevirapine to RT is found to decrease significantly upon enzyme mutation to K103N and further loss of energy to

*Correspondence to: J.Z.H. Zhang, Dept. of Chemistry, New York University, New York, NY 10003. E-mail: john.zhang@nyu.edu

Received 9 September 2004; Accepted 20 December 2004.

Published online 23 March 2005 in Wiley InterScience (www.interscience.wiley.com). DOI: 10.1002/prot.20455

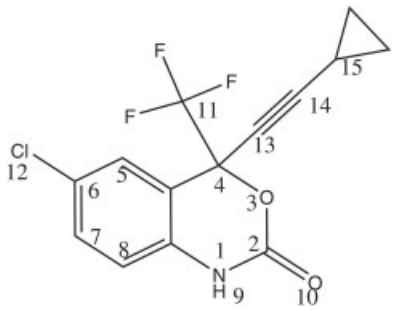

Fig. 1. Molecular structure of efavirenz (also named DMP-266, Sustiva, L-743,736).

Y181C. In this article, we apply the MFCC (molecular fractionation with conjugate caps) method to study binding of EFZ to HIV-1 RT and the mutants K103N and Y181C to understand the mechanism of EFZ binding. The MFCC method is linear scaling, computationally efficient, and particularly suitable for computing protein–ligand binding in which the protein remains fixed.

THEORY AND COMPOSITION

In the MFCC approach to computing interaction energy between EFZ and HIV-1 RT with a fixed structure, the enzyme is decomposed into amino acid fragments that are properly capped.[21] The MFCC method derives its great computational efficiency partly by foregoing calculations of intra-protein energy. In this study, we employ the MFCC method to compute binding interaction of EFZ to HIV-1 RT WT (wild type) and its mutants K103N and Y181C. The structure of EFZ is shown in Figure 1.

In MFCC calculation the enzyme is cut at peptide bonds along the backbone as shown in Figure 2(a). A pair of concaps (conjugate caps) (CH_3CO– and –$NHCH_3$) are inserted at each point of cut to cap the cutoff fragments as previously described[21,22] and illustrated in Figure 2(b). In addition to 922 fragments by cutting WT RT enzyme, there are also 921 concaps formed by the fusion of pairs of conjugate caps. Using the MFCC approach, the interaction energy for the EFZ-RT binding system (E_{L-RT}) is given by the following expression.[21]

$$E_{L-RT} = \sum_{i=1}^{N} E_{L,F_i} - \sum_{i=1}^{N-1} E_{L,CC_i} - \sum_{i=1}^{N} E_{F_i} + \sum_{i=1}^{N-1} E_{CC_i} - \sum_{i=1}^{Nd} E_{L,DC_i} + \sum_{i=1}^{Nd} E_{DC_i} + \sum_{i=1}^{Nd} E_L - E_L \quad (1)$$

where E_{L,F_i} denotes the ligand-ith fragment energy, E_{L,CC_i} the ligand-ith concaps (conjugate caps) energy, E_{F_i} and E_{CC_i} are, respectively, the self energy of the ith fragment and ith concaps and E_L is the ligand self energy. E_{L,DC_i} is the ligand-disulfide concaps energy as described in an earlier study.[23] The N and Nd are, respectively, the number of amino acids and disulfide bonds. For HIV-1 RT, there are no disulfide bonds ($Nd = 0$) and $N = 922$ for the WT enzyme.

The RT-EFZ complex structures are obtained from experimental crystal structures while positions of all hydrogen atoms are optimized using the Amber program[18] prior to computation of interaction energy. The MFCC calculations are carried out at HF, DFT, and MP2 levels in order to check the consistency of the results.

RESULTS AND DISCUSSION

Numerical Details

Three pdb files are used as initial EFZ-RT complex structures: 1FK9.pdb[24] for WT-EFZ, 1FK0.pdb[24] for K103N-EFZ, and 1JKH.pdb[25] for Y181C-EFZ. Hydrogen atoms are added and their positions are optimized using Amber7[26] with force field 99.[27] The EFZ is treated as a rigid body and minimized in the binding pocket. The residues in P66 are labeled from 1 to 560 and those in P51 are labeled from 561 to 1000. The interaction energies between EFZ and missing residues are set to zero.

Considering the computational cost, the MFCC calculation is first performed for all the fragment-EFZ interaction pairs at HF/3-21G level for the RT-EFZ complex with over 15,000 atoms. The MFCC calculation at this HF/3-21G level generates an enzyme-EFZ interaction spectrum as shown in Figure 3. The calculation is done using MPI for parallel execution on four P4/2.4 GHz linux PCS. As we can see from the interaction spectrum in Figure 3, the overwhelming majority of enzyme fragments have negligible interaction with the drug. For those fragment-EFZ pairs that show strong interactions, we further performed ab initio calculations at DFT B3LYP/6-31G* and MP2/6-31G* levels to verify the reliability of HF/3-21G calculation.

Table I lists the energies of the dominant enzyme fragment-EFZ interaction pairs for all three complex structures. The results in Table I show that HF/3-21G overestimates the binding energies of EFZ to Lys101 and Lys102, the two dominant binding residues in comparison to both B3LYP/6-31G* and MP2/6-31G*. The overestimation of hydrogen binding energy by HF/3-21G level of calculation is well expected. Besides this, the relative interaction profile for RT-EFZ interaction remains intact and the results obtained from different ab initio levels are consistent with each other.

EFZ Binding to Wild-Type HIV-1 RT

The root-mean-square distance (RMSD) of all atoms in RT-EFZ complex structure is 0.12 Å from the crystal structure after optimization in the binding pocket. The computed interaction spectrum at HF/3-21G level in Figure 3 shows that by far the predominant binding of EFZ is to the Lys101 residue. This is followed by much weaker bindings of EFZ to Lys102, Pro236, Asp237, and Leu100, etc. An interesting point to note is that there is a relatively strong repulsion between EFZ and Glu698. Figure 4 plots the relative positions of EFZ in complex with these residues with strong interaction reactions. By comparing results in Figure 3 and geometries in Figure 4, we explain binding character of EFZ to RT in the following. As can be seen from the geometries in Figure 4, the dominant

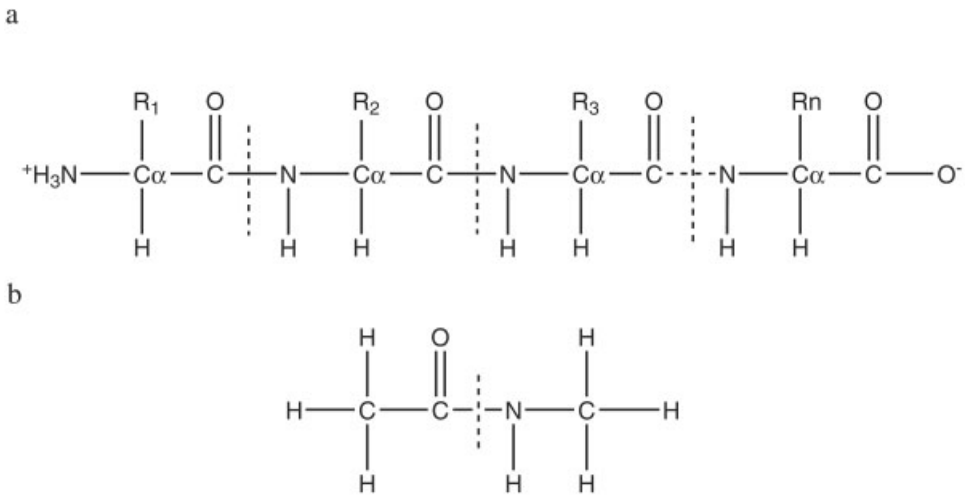

Fig. 2. **a:** Graphic representation of the locations of cuts in the MFCC approach. **b:** Cap and conjugate cap pair.

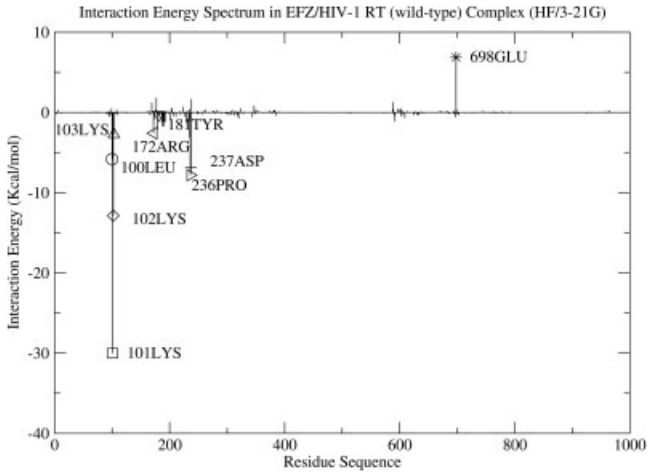

Fig. 3. MFCC computed interaction energy spectrum for EFZ/HIV-1 RT (wild-type) complex calculated at HF/3-21G.

bindings between EFZ and the Lys101 are from the following hydrogen bonding interactions: between the NH of EFZ and CO on the backbone of Lys101, between CO of EFZ and NH of Lys101. In addition, there is also an attractive interaction between CO of EFZ and the positively charged NH_3^+ side chain of Lys101. As shown in Figure 4, the distance between the corresponding oxygen atom of EFZ and the NH_3^+ in Lys101 is 5.18 Å, and thus produces an electrostatic attraction between them. These groups have quite favorable geometries for hydrogen-bonding-like interactions and they contribute about 30 kcal/mol binding energy from HF/3-21G calculation. The more reliable calculations at DFT B3LYP/6-31G* and MP2/6-31G* levels give an energy of around 21 kcal/mol for binding of EFZ to Lys101 as shown in Table I. This is essentially equivalent to the strength of two strong hydrogen-bonds. Thus strong binding of EFZ to Lys101 is the primary mechanism of drug binding to RT. This is in clear contrast to the first-generation drug nevirapine which does not have any strong hydrogen bonding to RT.[15]

In addition to the predominant binding to Lys101 residue, EFZ also has significant attractive interactions with Lys102 and to a lesser degree with Asp237, Pro236, and Leu100 as shown in Figure 4. Table I lists the interaction energies between EFZ and these residues computed at HF/3-21G, B3LYP/6-31G*, and MP2/6-31G* levels. As is quite consistent that HF/3-21G overestimates the binding binding in comparison to B3LYP/6-31G* and MP2/6-31G* results as shown clearly in Table I. Similar trend is seen in Table I that the the binding energy energy of Lys102, Pro236, and Leu100 are much reduced as shown in Table I. They contribute to binding energy in the range of a few kcal/mol but do not form any strong hydrogen bonds with EFZ as is consistent with the geometric positions shown in Figure 4.

The present MFCC calculation predicts the existence of a repulsive interaction between EFZ and residue Glu698 as shown in the interaction spectrum of Figure 3. Calculation at all three levels gives a consistent energy around 6 kcal/mol. Examination of the relative geometry in Figure 4 shows that the CO group of EFZ lies only 4.1 Å away from the negatively charged carboxyl group of Glu698. This is believed to be responsible for this repulsion.

EFZ Binding to K103N Mutant

The K103N mutation in which Lys103 is replaced by Asn103 is a major mutant in HIV-1 RT that exists in over 90% of the patients who developed drug resistance after initial treatment of NNRTIs.[28–31] According to the study, the K103N mutant shows a six-fold loss of binding to EFZ compared to WT RT.[16] We use the crystal structure[24] as the starting structure and similar numerical procedures are followed. The optimized complex structure in the binding pocket has RMSD of 0.24 Å. Figure 5 plots the interaction spectrum generated from the MFCC calculation at HF/3-21G level for EFZ-K103N binding.

A few things are changed in the mutant-EFZ complex. First, the K103N mutation causes relatively large conformational rearrangement within the binding pocket com-

TABLE I. Interaction Energies Between EFZ and Selected Amino Fragments (Capped) of HIV-1 RT and its Mutants From Different Levels of ab initio Calculations

	Interaction energy (Kcal/mol)								
	Wild type			K103N			Y181C		
Residue	HF	B3LYP	MP2	HF	B3LYP	MP2	HF	B3LYP	MP2
LEU100	−5.83	−3.64	−1.49	−6.84	−3.85	−0.88	−4.61	−2.20	0.62
CAP100	−4.62	−4.62	−4.11	−7.77	−5.37	−4.41	−4.81	−3.79	−3.10
LYS101	−30.00	−21.86	−21.02	−26.71	−17.98	−16.55	−31.26	−22.60	−21.44
CAP101	−11.28	−8.30	−10.06	−16.22	−10.39	−9.18	−16.86	−10.79	−9.17
LYS102	−12.87	−7.82	−6.17	−11.94	−6.92	−5.28	−12.27	−6.94	−5.03
LYS103	−2.74	−2.60	−1.60	1.93 (ASN)	0.59 (ASN)	1.69 (ASN)	−2.85	−2.79	−1.87
TYR181	−0.28	−0.33	0.34	−1.62	−1.10	0.17	0.74 (CYS)	0.75 (CYS)	2.54 (CYS)
PRO236	−7.82	−3.65	−2.25	−5.91	−3.50	−3.12	−6.33	−3.91	−3.52
ASP237	−6.86	−5.80	−5.16	−5.01	−4.41	−4.20	−4.25	−3.95	−3.62
GLU698	6.86	5.47	6.76	4.12	3.18	3.89	10.78	7.84	10.25

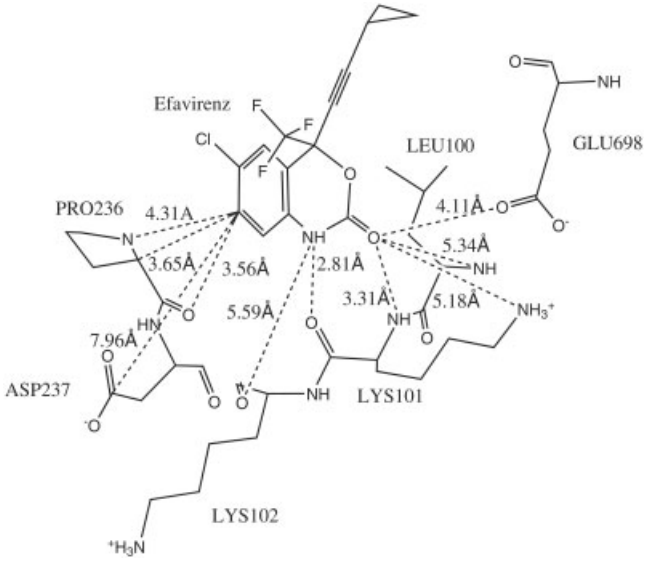

Fig. 4. Relative geometries and distances of EFZ and HIV-1 RT fragments in EFZ/HIV-1 RT (wild-type) complex.

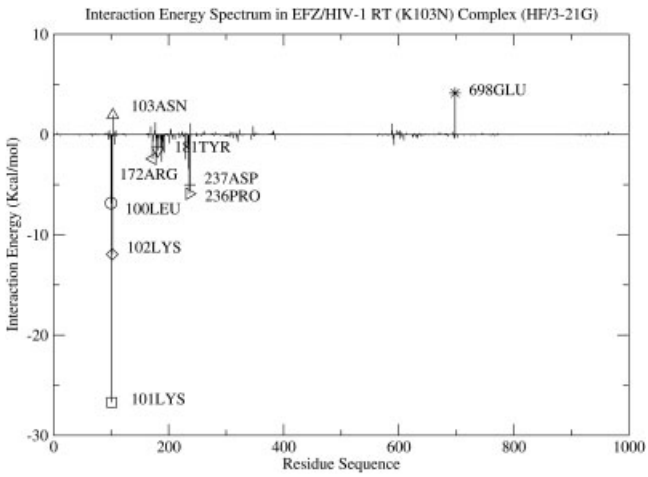

Fig. 5. Similar to Figure 3 except for K103N.

pared with the WT RT. The displacement of EFZ itself within the binding site is very limited.[24] For the dominant binding pair, the two hydrogen-bonding-like interactions between EFZ and LYS101 are not changed much compared with the WT enzyme. However, the charged residue NH_3^+ in LYS101 is now 6.87 Å, much larger than the 5.18 Å in the WT. As a result, the binding energy between EFZ and K103N is reduced by about 4 kcal/mol as can be shown in Figure 6 and in Table I. However, the tight binding of EFZ to Lys101 has not been significantly weakened.

Next, the replacement of Lys103 by Asn103 creates a repulsion between EFZ and Asn103 with a repulsion energy of less than 2 kcal/mol (cf. Fig. 4 and Table I). The change from the methylene group of lysine to the bulk of amide group of asparagine causes the side chain of Tyr181 flip to a "down" orientation, which pushes Glu698 away from the binding pocket and is about 2.48 Å away from EFZ relative to the WT. This results in a decrease of repulsive energy by about 3.20 kcal/mol relative to the WT (cf. Figs. 4–5 and Table I).

Thus the main effect in K103N mutation is that the dominant binding interaction between EFZ and Lys101 is slightly weakened by about 4 kcal/mol due to the increase of distance between the CO group of EFZ and the NH_3^+ group in Lys101. This is the main conclusion from the MFCC calculation for EFZ binding to K103N. The current computational analysis provides an explanation for drug resistance of K103N mutation in terms of binding interaction energy based on crystal structure of the complex. This explanation is complementary to an experimental suggestion that K103N mutation stabilizes the closed form of RT and therfore reduces the rate of inhibitor entry.[32] However, the vastly improved resistance of Efavirenz to K103N mutation (six-fold binding loss) than that of the first generation drug Nevirapine (40-fold binding loss) provides clear evidence that drug-resistance of K103N mutation depends on specific drug binding interactions.

EFZ Binding to Y181C Mutant

Mutation at Tyr181 has been frequently reported in resistance studies and the change is almost always to cysteine.[14] EFZ shows a 2.5-fold reduction in binding to this mutant RT.[16] We follow the same numerical proce-

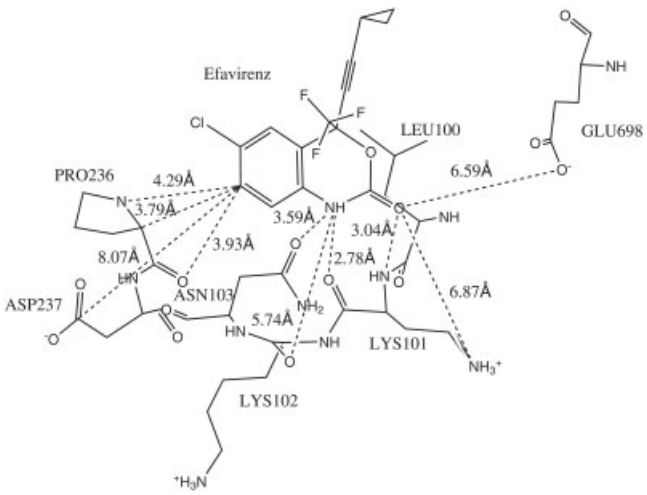

Fig. 6. Similar to Figure 4 except for K103N.

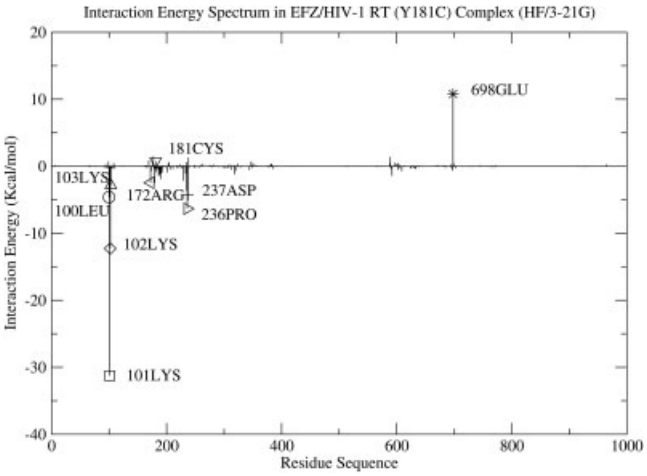

Fig. 7. Similar to Figure 3 except for Y181C.

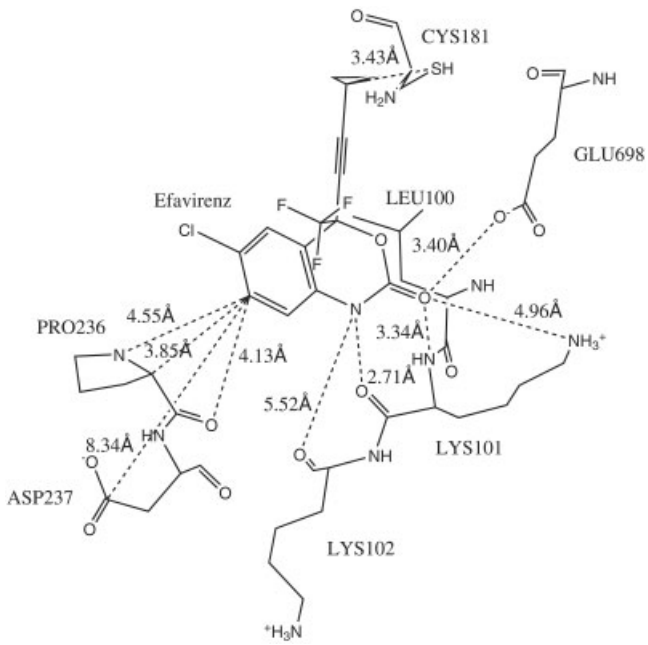

Fig. 8. Similar to Figure 4 except for Y181C.

TABLE II. MFCC Computed Binding Energies (kcal/mol) of EFZ to WT, K103N and Y181C Mutants of RT at HF/3-21G Level in Comparison with Experimentally Observed Binding Loss of EFZ on Mutations

Efavirenz	WT	K103N	Y181C
MFCC binding energy	52	48	49
Experiment binding loss	1	Six-fold	2.5-fold

dure as described previously to perform the MFCC calculation. The RMSD from the crystal structure (pdb id 1JKH) is 0.32 Å. The computed interaction energy spectrum is shown in Figure 7 and the relative geometry is shown in Figure 8.

From the interaction spectrum in Figure 7 and Table I, we notice that a major effect of Y181C mutation is that the Glu698 residue moves closer to EFZ, from 4.1 Å in WT to 3.4 Å (cf. Figs. 4, 8), resulting in an increase of repulsive energy by 3–4 kcal/mol, relative to the WT. This is what we believe is the main cause of weakened binding of EFZ to Y181C. Besides this, the main binding between EFZ and Lys101 is essentially conserved in comparison to that in the WT.

With Tyr181 mutation to Y181C, the phenol in Tyr181 is replaced by the polar SH group, which breaks the hydrophobic environment around the cyclopropyl group of EFZ. Because the distance between C15 of EFZ and the sulfur atom of Y181C is only 3.43 Å, there is a small increase of repulsion between EFZ and Cys181 in comparison to the WT. The interactions of EFZ to Lys103, Pro236, and Asp237 remains similar to those in WT.

Table II shows a comparison of binding effect of EFZ to RT and its mutants between MFCC calculated binding energy and experimentally observed binding loss. The computed binding energy of EFZ to RT drops by 4 and 3 kcal/mol upon mutation to K103N and Y181C, respectively, which is in quite good agreement with the experimentally observed corresponding binding loss of six-fold and 2.5-fold. Although absolute binding energies calculated at HF/3-21G level may have relatively large errors, the *relative* binding energies of EFZ to different mutant RTs are expected to be reasonably reliable. This is consistent with the fact that HF method is widely used for molecular structure optimization despite large errors in its calculated absolute energies.

DPC961 Binding to RT

DPC961 is also a second generation nonnucleoside reverse transcriptase inhibitor (NNRTI) in which the benzoxazine ring of the FDA-approved NNRTI efavirenz has been replaced with a quinoxaline ring as shown in Figure 9. In vitro, DPC 961 strongly inhibits HIV-1 and more importantly inhibits NNRTI drug-resistance isolates significantly better than efavirenz.[33,34] Because the molecu-

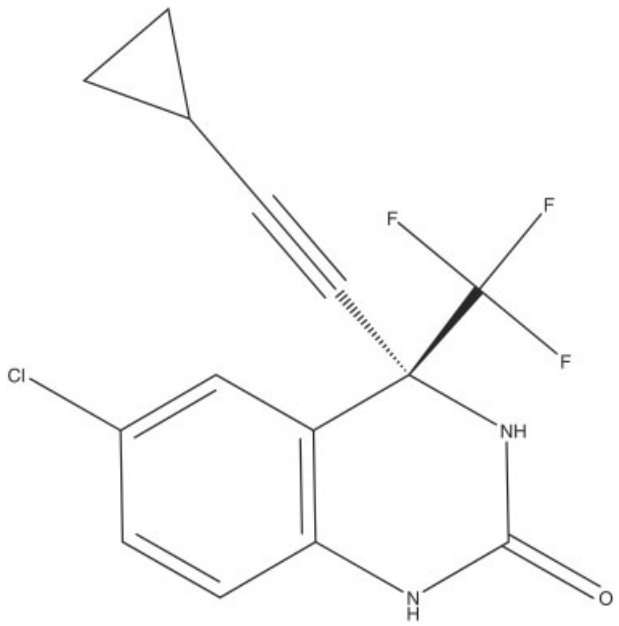

Fig. 9. Molecular structure of DPC961.

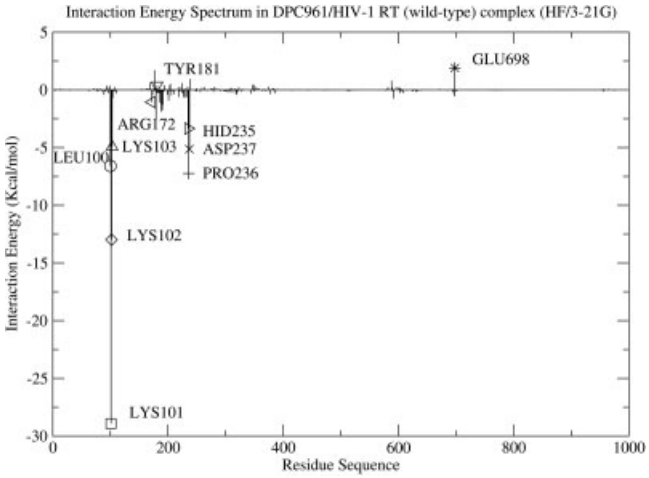

Fig. 10. MFCC-computed interaction energy spectrum for DPC961/HIV-1 RT (wild-type) complex calculated at HF/3-21G.

lar structure of DPC961 is very close to EFZ, we also carried out MFCC calculation to study its binding to RT and mutants.

For RT-DPC961, we do not have the crystal structure of the protein binding complex available. However, due to similarity of its structure to EFZ, we placed DPC961 into the binding pocket with nearly the same position and orientation as EFZ in RT. We then optimized the position and orientation of DPC961 and of hydrogen atoms in the complex using AMBER force field. The RMSD of heavy atoms in DPC961 is 0.18 Å relative to EFZ, which suggests that the binding geometry and orientation of both drugs are very similar.

Figure 10 shows the interaction spectrum of DPC961 binding to HIV-1 RT (wild type). Comparing Figure 10 with the interaction spectrum for EFZ-RT in Figure 3, we see that binding of DPC 961 to RT is enhanced by the following mechanism. First, there is an additional attractive interaction which is between DPC961 and residue Hid235 although it is relatively weak. Secondly, the repulsion between Glu698 and the drug has been substantially reduced. The overall binding energy of DPC961 to WT RT is −55 kcal/mol at HF/3-21G level, which is about 4 kcal/mol larger than that of EFZ binding to WT RT. Thus, DPC691 seem to be a better inhibitor in terms of binding to HIV-1 RT.

DISCUSSION AND CONCLUSION

The MFCC method has been applied to study binding of EFZ to HIV-1 RT and two major mutants, K103N and Y181C at HF, DFT, and MP2 levels of calculation. The quantum mechanical MFCC calculation shows that EFZ binds predominantly to the Lys101 residue of RT through strong electrostatic interactions, between the NH of EFZ and CO of Lys101; between CO of EFZ and NH and the positively charged NH_3^+ side chain of Lys101. There is a prominent repulsion between EFZ and the residue Glu698 due to the close distance between them. In K103N mutant, the dominant binding of EFZ to Lys101 is slightly weakened due to conformational change of the binding complex that results in the NH_3^+ group in Lys101 being moved further away from the CO atom of EFZ. In addition, the replacement of Lys103 by Asn103 creates a small repulsion between EFZ and Asn103. This is consistent with the sixfold loss of binding EFZ to K103N observed experimentally. In Y181C mutant, the EFZ binding to Y181C is slightly weakened due primarily to the stronger repulsion between EFZ and Glu698 relative to the WT. This is consistent with the experimentally observed 2.5-fold of loss of binding to Y181C mutation by EFZ. The EFZ-derived DPC961 is shown to have tighter binding to RT by about 4 kcal/mol due partially to the reduction of repulsive energy between EFZ and Glu698.

Current computational study of mutation effect could provide us the following insight, which could be useful in designing more mutation resistant inhibitors. For example, it is important for the potential inhibitors to have relatively strong attractive interactions (such as hydrogen bonding) to those residues that are conserved upon mutations. In EFZ binding to RT, we see that the dominant binding is to Lys101 which is conserved in K103N and Y181C mutations. This could explain the much improved mutation-resistant property of EFZ compared to the first-generation drug Nevirapine. On the other hand, it is not hard to imagine that if a mutation involves Lys101, the binding effect of EFZ could be seriously impacted.

It should be noted that in current study, solvent is not explicitly included and therefore the absolute binding interaction energy could not be compared to experimentally observable binding free energy. However, the relative difference of binding interaction energy between the drug molecule and different mutants of HIV-1 RT is quite meaningful. Current methods for free energy calculation of protein–drug binding are extremely difficult and computationally expensive. More importantly, the error bars from

such free energy calculations are usually too large to enable quantitative determination of relatively free energy of binding, especially when the difference is small. Thus the purpose of the current work is not to give quantitative prediction of free energy of binding to mutants, but to provide a qualitative and mechanistic explanation of mutational effect from detailed analysis of molecular interaction. This will provide insight on the nature of mutational effect and aid the future design of better inhibitors.

REFERENCES

1. Parker WB, White EL, Shaddix SC, Ross LJ, Buckheit RW Jr, Germany JM, Secrist JAd, Vince R, Shannon WM, Mechanism of inhibition of human-immunodeficiency-virus type-1 reverse-transcriptase and human DNA polymerase-alpha, polymerase-beta, and polymerase-gamma by the 5′-triphosphates of carbovir, 3′-azido-3′-deoxythymidine, 2′,3′-dideoxyguanosine, and 3′-deoxythymidine—a novel RNA template for the evaluation of antiretroviral drugs. J Biol Chem 1991;266:1754–1762.
2. Kohlstaedt LA, Wang J, Friedman JM, Rice PA, Steitz TA. Crystal-structure at 3.5 Å resolution of HIV-1 reverse-transcriptase complexed with an inhibitor. Science 1992;25:1783–1790.
3. Rizzo RC, Tirado-Rives J, Jorgensen WL. Estimation of binding affinities for HEPT and nevirapine analogues with HTV-1 reverse transcriptase via Monte Carlo simulations. J Med Chem 2001;44: 145–154.
4. Mitsuya H, Yarchoan R, Broder S. Molecular targets for aids therapy. Science 1990;249:1533–1544.
5. Katz RA, Skala AM. The retroviral enzymes. Ann Rev BioChem 1994;63:133–173.
6. Wang J, Morin P, Wang W, Kollman PA. Use of MM-PBSA in reproducing the binding free energies to HIV-1 RT of TIBO derivatives and predicting the binding mode to HIV-1 RT of efavirenz by docking and MM-PBSA. J Am Chem Soc 2001;123: 5221.
7. Esnouf R, Ren J, Ross C, Jones Y, Stammers D, Stuart D. Mechanism of inhibition of HIV-1 reverse-transcriptase by non-nucleoside inhibitors. Nat Struct Biol 1995;2:303–308.
8. Kopp EB, Miglietla JJ, Shrutkowski AG, Shih CK, Grob PM, Skoog MT. Steady state kinetics and inhibition of HIV-1 reverse transcriptase by a nonnucleoside dipyridodiazepinone, BI-RG-587, using a heteropolymeric template. Nature 1991;19:3035–3039.
9. Romero DL, Bussa M, Tan CK, Reusser F, Palmer JR, Poppe SM, Aristoff PA, Downery KM, So AG, Resnick L, and others. Non-nucleoside reverse transcriptase inhibitors that potently and specifically block human immunodeficiency virus type 1 replication, Proc Natl Acad Sci USA 1991;88:8806–8810.
10. Archer RH, Wisniewski M, Bambara RA, Demeter LM. The Y181C mutant of HIV-1 reverse transcriptase resistant to nonnucleoside reverse transcriptase inhibitors alters the size distribution of RNase H cleavages. Biochemistry 2001;40:4087.
11. De Clerco E. Nonnucleoside reverse transcriptase inhibitors (NNRTIs) for the treatment of human immunodeficiency virus type 1 (HIV-1) infections: strategies to overcome drug resistance development. Med Res Rev 1996;16:125–157.
12. Jonckheere H, Anne J, De Clercq E. The HIV-1 reverse transcription (RT) process as target for RT inhibitors. Med Res Rev 2000;2:129–154.
13. Bacheler LT. Resistance to nonnucleoside inhibitors of HIV-I reverse transcriptase. Drug Resist Updates 1999;2:56.
14. Schinazi RF, Larder BA, Mellors JW, Mutations in retroviral genes associated with drug resistance. Int Antiviral News 1997;5: 129–142.
15. He X, Mei Y, Xiang Y, Zhang DW, Zhang JZH. Proteins (accepted).
16. Young SD, Britcher SF, Tran LO, Payne LS, Lumma WC, Lyle TA, Huff JR, Anderson PS, Olsen DB, Carroll SS, Pettibone DJ, O'Brien JA, Ball RG, Balani SK, Lin JH, Chen IW, Schleif WA, Sardana VV, Long WJ, Byrnes VW, Emini EA. L-743,726 (DMP-266): a novel, highly potent nonnucleoside inhibitor of the human immunodeficiency virus type 1 reverse transcriptase. Antimicrob Agents Chemother 1995;39:2602–2605.
17. Rizzo RC, Wang DP, Tirado-Rives J, Jorgensen, William L. Validation of a model for the complex of HIV-1 reverse transcriptase with sustiva through computation of resistance profiles. J Am Chem Soc 2000;122:12898.
18. Wang JM, Morin P, Wang W, Kollman PA. Use of MM-PBSA in reproducing the binding free energies to HIV-1 RT of TIBO derivatives and predicting the binding mode to HIV-1 RT of efavirenz by docking and MM-PBSA. J Am Chem Soc 2001;123: 5221.
19. Rizzo RC, Udier-Blagovic M, Wang DP, Watkins EK, Smith MBK, Smith RH, Tirado-Rives J, Jorgensen WL. Prediction of activity for nonnucleoside inhibitors with HIV-1 reverse transcriptase based on Monte Carlo simulations. J Med Chem 2002;45:2970–2987.
20. Kuno M, Hannongbua S, Morokuma K. Theoretical investigation on nevirapine and HIV-1 reverse transcriptase binding site interaction, based on ONIOM method. Chem Phys Lett 2003;380:456.
21. Zhang DW, Zhang JZH. Molecular fractionation with conjugate caps for full quantum mechanical calculation of protein-molecule interaction energy. J Chem Phys 2003;119:3599.
22. Zhang DW, Xiang Y, Gao AM, Zhang JZH. Quantum mechanical map for protein-ligand binding with application to beta-trypsin/benzamidine complex. J Chem Phys 2004;120:1145.
23. Chen XH, Zhang DW, Zhang JZH. Fractionation of peptide with disulfide bond for quantum mechanical calculation of interaction energy with molecules. J Chem Phys 2004;120:839–844.
24. Ren J, Milton J, Weaver KL, Short SA, Stuart DI, Stammers DK. Structural basis for the resilience of efavirenz (DMP-266) to drug resistance mutations in HIV-1 reverse transcriptase. Structure 2000;8:1089.
25. Ren J, Nichols C, Bird L, Chamberlain P, Weaver K, Short S, Stuart DI, Stammers DK. Structural mechanisms of drug resistance for mutations at codons 181 and 188 in HIV-1 reverse transcriptase and the improved resilience of second generation non-nucleoside inhibitors. J Mol Biol 2001;312:795.
26. Pearlman DA, Case DA, Caldwell JW, Ross WS, Cheatham TE III, DelBolt S, Ferguson D, Seibel G, Kollman P. AMBER, a package of computer-programs for applying molecular mechanics, normal-mode analysis, molecular-dynamics and free-energy calculations to simulate the structural and energetic properties of molecules. Comput Phys Commun 1995;91:1–41.
27. Wang J, Cieplak P, Kollman PA. How well does a restrained electrostatic potential (RESP) model perform in calculating conformational energies of organic and biological molecules? J Comput Chem 2000;21:1049.
28. Bacheler L, Jeffrey S, Hanna G, D'Aquila R, Wallace L, Logue K, Cordova B, Hertogs K, Larder B, Buckery R, and others. Genotypic correlates of phenotypic resistance to efavirenz in virus isolates from patients failing nonnucleoside reverse transcriptase inhibitor therapy. J Virol 2001;75:4999–5008.
29. Miller V, Sturmer M, Staszewski S, Groschel B, Hertogs K, de Bethune MP, Pauwels R, Harrigan PR, Bloor S, Kemp SD, and others. The M184V mutation in HIV-1 reverse transcriptase (RT) conferring lamivudine resistance does not result in broad cross-resistance to nucleoside analogue RT inhibitors. AIDS 1998;12: 705.
30. Torti C, Pozniak A, Nelson M, Hertogs K, Gazzard BG. Distribution of K103N and/or Y181CHIV-1 mutations by exposure to zidovudine and non-nucleoside reverse transcriptase inhibitors. J Antimicrob Chemother 2001;48:113.
31. Conway B, Wainberg MA, Hall D, Harris M, Reiss P, Cooper D, Vella S, Curry R, Robinson P, Lange JM, and others. Development of drug resistance in patients receiving combinations of zidovudine, didanosine and nevirapine. AIDS 2001;15:1269.
32. Yu H, Ding J, Das K, Clark AD Jr., Boyer PL, Lewi P, Janssen PA, Lleim J, Rosner M, Hughes SH, and others. The Lys103Asn mutation of HIV-1 RT: a novel mechanism of drug resistance, J Mol Biol 2001;309:437.
33. Jeffrey S, Baker D, Corbett J, Logue K, BACHELER LT, resistance profile of four second-generation NNRTI candidates (Abstract 1172), 39th interscience conference on antimicrobial agents and chemotherapy. 1999;39:495.
34. Corbett JW, Ko SS, Rodgers JD, Bacheler LT, Klabe RM, Diamond S, Lai CM, Rabel SR, Saye JA, Adams SP, and others. Expanded-spectrum nonnucleoside reverse transcriptase inhibitors inhibit clinically relevant mutant variants of human immunodeficiency virus type 1. Antimicrob Agents Chemother 1999;43:2893–2897.